Computational Study of a New Heck Reaction Mechanism Catalyzed by Palladium(II/IV) Species

Andreas Sundermann, Olivier Uzan, and Jan M. L. Martin*[a]

Abstract: In this theoretical study on the Heck reaction we explore the feasibility of an alternative pathway that involves a Pd^{II}/Pd^{IV} redox system. Usually, the catalytic cycle is formulated based on a Pd^{0}/Pd^{II} mechanism. We performed quantum chemical calculations using density functional theory on a model system that consisted of diphosphinoethane (DPE) as a bidentate ligand and the substrates ethylene and phenyl iodide to compare both mechanisms. Accordingly, the Pd^{II}/Pd^{IV} mechanism is most likely to occur in the equatorial plane of an octahedral Pd^{IV} complex. The energy profiles of both reaction pathways under consideration are largely parallel. A major difference is found for the oxidative addition of the C–I bond to the palladium centre. This is a rate-determining step of the Pd^{II}/Pd^{IV} mechanism, while it is facile for a Pd^{0} catalyst. The calculations show that intermediate ligand detachment and reattachment is necessary in the course of the oxidative addition to Pd^{II}. Therefore, we expect the Pd^{II}/Pd^{IV} mechanism to be only feasible if a weakly coordinating ligand is present.

Keywords: density functional calculations · Heck reaction · homogeneous catalysis · reaction mechanisms

Introduction

The Heck reaction (i.e., the palladium catalysed olefination of aryl halides, Scheme 1) has become an important tool for the formation of C–C bonds in organic synthesis.[1–3]

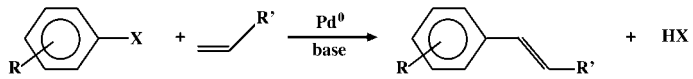

Scheme 1. The Heck reaction.

In the "standard" Heck reaction, the catalytically active complex is formed in situ (starting from palladium(0) complexes or palladium(II) salts). Although its molecular structure is not exactly known, a coordinative unsaturated 14-electron palladium(0) complex "$[PdL_2]$" is assumed to be the active species. The ligand "L" is typically either a monodentate phosphine or part of a chelating diphosphine ligand. Usually, the reaction mechanism is described as in Scheme 2.

In a first step the C–X bond of an aryl halide (X = I, Br) is oxidatively added to the palladium atom. The resulting square planar palladium(II) complex has to dissociate (either by Pd–L

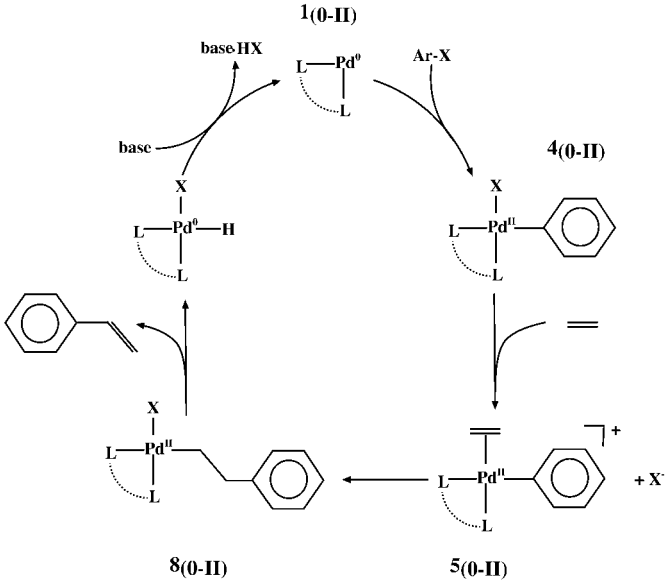

Scheme 2. Heck catalytic cycle with $Pd^{(0/II)}$ redox pair.

[a] Dr. J. M. L. Martin, Dr. A. Sundermann, O. Uzan
Department of Organic Chemistry, Kimmelman Building
Room 262, Weizmann Institute of Science
76100 Rehovot (Israel)
Fax: (+9728) 934 4142
E-mail: comartin@wicc.weizmann.ac.il

Supporting information for this article is available on the WWW under http://www.wiley-vch.de/home/chemistry/ or from the author. Cartesian coordinates in XMOL ("*xyz*") format, absolute energies and harmonic frequencies for all stationary points are available in machine-readable format on the Internet World Wide Web at the Uniform Resource Locator http://theochem.weizmann.ac.il/web/papers/heck.html. Molecular animations of the IRCs of key reaction steps are available at the same location.

  0947-6539/01/0708-1703 $ 17.50+.50/0

or Pd–X bond breaking) to provide a coordination site for alkene association. If the alkene and the σ-aryl ligand are in *cis* positions, the alkene can insert into the Pd–C_{ar} bond. Via a four-centred transition state, a *σ*-alkyl palladium complex is formed. This intermediate is converted into the reaction product by a *β*-hydride elimination, and the catalyst is regenerated after HX elimination in the presence of an auxiliary base. (The Heck reaction is typically carried out in highly polar solvents such as dimethylformamide, *N*-methylpyrrolidone and dimethylacetamide.)

Recently, very high activities and long lifetimes have been reported for new palladium catalysts for the Heck reaction.[4–14] In these studies, structurally well-defined species have been used that contain palladacycles with phosphine groups **A**,[4] or with phosphine-free ligands **B**.[11]

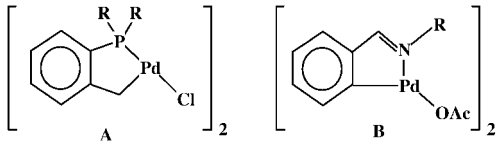

Because these complexes have a palladium(II) centre and no palladium(0) species could be detected in the reaction mixture, a new reaction mechanism involving a Pd^{II}/Pd^{IV} redox pair (instead of the usual Pd^0/Pd^{II} pair) has been proposed. An experimental proof for the reaction mechanism is difficult because of the elusive nature of the active species. Therefore we want to contribute computational results demonstrating that a Pd^{II}/Pd^{IV} route is energetically competitive to the "classical" mechanism.

A possible mechanism involving the Pd^{II}/Pd^{IV} system is depicted in Scheme 3. The catalytic cycle begins with a cationic T-shaped palladium(II) complex. As in the Pd^0/Pd^{II} mechanism, this complex fragment is a 14-electron species, but it is formally a d^8 fragment (instead of a d^{10} configuration as in the Pd^0 complex). Oxidative addition of an aryl halide and alkene coordination results in an octahedrally coordinated palladium atom that formally has a d^6 configuration. If

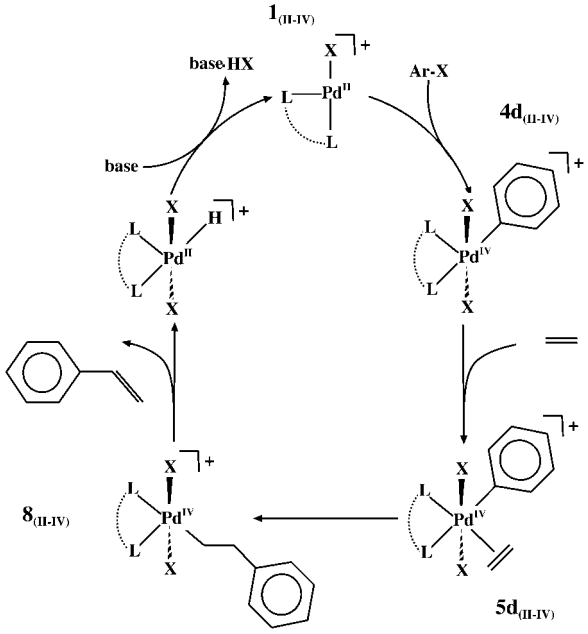

Scheme 3. Heck catalytic cycle with $Pd^{(II/IV)}$ redox pair.

the phenyl group and the alkene are in a mutual *cis* arrangement, the alkene can insert into the Pd–C_{ar} bond as assumed for the "classical" mechanism. Now, *β*-hydride elimination can take place. The product is released and the catalyst is regenerated by HX elimination.

Essentially, the two mechanisms are expected to involve identical reaction steps. The question we want to address in this study is: Are the corresponding barriers of comparable height, that is, is the suggested Pd^{II}/Pd^{IV} mechanism of the Heck reaction a possible alternative to the Pd^0/Pd^{II} mechanism?

Abstract in Hebrew:

בחקירה תיאורטית הזאת בנושא "תגובת הק" אנחנו בוחנים את סבירותו של מסלול תגובה אלטרנטיבי שמבוסס על זוג חימצון-חיזור Pd II/IV. כדי להשוות את שני המנגנונים, ביצענו חישובים כימיים קוונטים באמצעות תורת פונקציונל הצפיפות על מערכת מודל שמורכב מדיפוספינואתאן כלינגד דו-זרועי, ואתילן ויודובנזן כסובסטרטים. לפי החישובים האלה, המנגנון Pd II/IV הכי צפוי לקרות במישור האקוואטוריאלי של קומפלקסים אוקטהדרלים של Pd(IV). פרופילי האנרגיה של שני מסלולי התגובה השקולים הם במידה רבה מקבילים. אולם נמצא הבדל מהותי לסיפוח מחמצן של קשר C-I ל- Pd. זהו השלב הקובע מהירות של המנגנון Pd(II/IV); אולם לקטליזטור Pd(II). לכן צפוי שהמנגנון Pd(II/IV) סביר רק אם נמצא ליגנד בעל קואורדינציה חלשה למתכת.

Computational Methods

All structures presented here were completely optimised at the density functional theory (DFT) level by using the B3LYP hybrid functional proposed by Becke[15] as implemented in the Gaussian 98 set of programs.[16] For all optimisations a basis set of valence double-*ζ* quality was employed. Relativistic effects were addressed implicitly by the use of relativistic effective core potentials (RECPs) for P, I and Pd.[17–19] For H and C the standard Dunning–Hay D95V basis was used.[20] This basis set/RECP combination is commonly denoted by the acronym "lanl2dz".

Although most of the molecules included in this study adopt C_1 symmetry—and therefore no symmetry constraints could be applied—all stationary points were characterised by analysis of the analytically calculated Hessians. Estimates for ΔG(298 K) and ΔH(298 K) have been calculated within the rigid rotor/harmonic oscillator (RRHO) approximation. In ambiguous cases for which an assignment by inspection of the corresponding imaginary eigenmode was not obvious, the correct topology of the potential energy hypersurface was verified by calculation of the intrinsic reaction coordinate (IRC)[21] at the B3LYP/lanl2dz level.

In order to obtain more reliable thermochemical data, additional single-point energy calculations were performed at the B3LYP/lanl2dz + p and the B3LYP/B_{large} level. The basis set lanl2dz + p consisted of the lanl2dz basis set augmented by a single d polarisation function for P and I and a single f polarisation function for palladium.[22, 23] For H and C the cc-pVDZ basis of Dunning was used.[24] The basis set "B_{large}" was essentially a polarised (i.e., 2f1g, 2d1f, 2p1d) valence triple-*ζ* basis set. For the atoms H, C and P the cc-pVTZ basis set of Dunning[24, 25] was recontracted according

0947-6539/01/0708-1704 $ 17.50+.50/0 *Chem. Eur. J.* **2001**, *7*, No. 8

to Davidson[26]; for Pd and I the Stuttgart/Dresden small core RECPs[27, 28] were utilised. A [6s5p3d] contraction of the (8s7p6d) primitive set for Pd was taken from the literature[27] and supplemented with two f and one g polarisation functions optimised at the CISD level for the electronic ground state ($\zeta_f = 0.6122$, 2.1857; $\zeta_g = 1.3751$). The valence basis set for I was generated in our laboratory: Even-tempered sequences ($\zeta = \alpha\beta^{k-1}$) with six s ($\alpha = 0.106898$, $\beta = 2.388398$) and six p ($\alpha = 0.082252$, $\beta = 2.602393$) primitives were optimised at the SCF level for the ^{2}P state, and contracted to a [3p3s] set in a [411] pattern. Two d and one f polarisation functions were optimised at the CISD level ($\zeta_d = 0.1861$, 0.3637, $\zeta_f = 0.4279$), again for the ^{2}P state. Symmetry and spin restrictions were imposed during these calculations, which were carried out by using MOLPRO.[29]

Because of the known deficiencies of the B3LYP density functional for predicting barrier heights,[30] we verified our results by single-point calculations using the *m*PW1PW91 functional by Adamo and Barone[31] with the lanl2dz + p basis set.

To ensure reproducibility of all computed data, all DFT calculations were carried out with finer grids than the defaults: specifically, following the recommendations in reference [32], a pruned (99, 590) grid was used for energies and gradients, and (in frequency calculations) a pruned (50, 194) grid for the coupled perturbed Kohn–Sham step.[33] The default pruned (95, 302) grid was employed only for the largest basis set single-point calculations, in order to keep the computational cost to an acceptable level.

For all calculations the Gaussian 98 set of programs[16] was used, running on the SGI Origin 2000 of the Faculty of Chemistry of the Weizmann Institute and on SGI Octane, Compaq XP1000, and Compaq ES40 workstations in our laboratory. The structures were visualised using the program MOLDEN 3.6.[34]

Results and Discussion

We performed quantum chemical calculations on a model system consisting of the bidentate 1,2-diphosphinoethane (DPE) ligand and the substrates phenyl iodide and ethylene to model the steps of the "classical" Heck reaction (Scheme 2). For the Pd^{II}/Pd^{IV} pathway (Scheme 3) an additional ligand is required to take into account that the preferred coordination number for a Pd^{IV} centre is six rather than four (as in the square-planar coordination found for Pd^{II} complexes). In order to minimise the number of possible isomers we chose I^- for this purpose.

Only recently a theoretical study has been published by Albert, Gisdakis, and Rösch[35] on the Pd^0/Pd^{II} mechanism. These authors modelled the catalytic cycle involving a carbene-stabilised palladium centre. Although our results for the Pd^0/Pd^{II} mechanism are very similar, we report them here together with the Pd^{II}/Pd^{IV} catalytic cycle to allow a comparison between the two pathways for one system without changing the ligands.

The active catalyst: The active catalyst for the Pd^0/Pd^{II} pathway is anticipated to be a neutral, C_2 symmetric DPE-palladium(0) complex. Our calculations result in a Pd–P bond length of 2.400 Å and a P-Pd-P bond angle of 94.3° for this structure. The carbon atoms are twisted out of the P-Pd-P plane by 11.0° to allow a strain-free, staggered conformation of the ethane backbone. Complex $\mathbf{1}_{(0\text{-}II)}$ is capable of σ bonding and π back-bonding towards an additional ligand approaching the palladium atom along the symmetry axis. This can be demonstrated by a plot of the frontier orbitals (Figure 1).

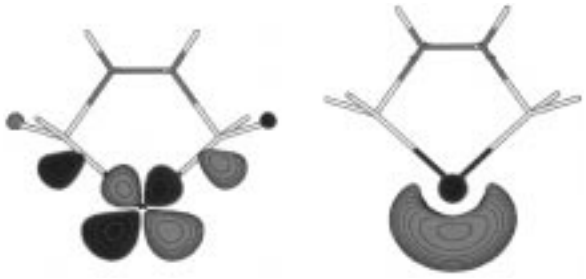

Figure 1. Isosurface representation of the frontier orbitals of Pd(dpe). Left: HOMO, B symmetry, right: LUMO, A symmetry (assignments according to point group C_2)

Thus, η^2-ethylene as well as (C–C) η^2-phenyl iodide complex formation is possible in the presence of these substrate molecules (for the corresponding structures $\mathbf{2}_{(0\text{-}II)}$ and $\mathbf{3}_{(0\text{-}II)}$ see Figure 2). Ethylene is bound more strongly by

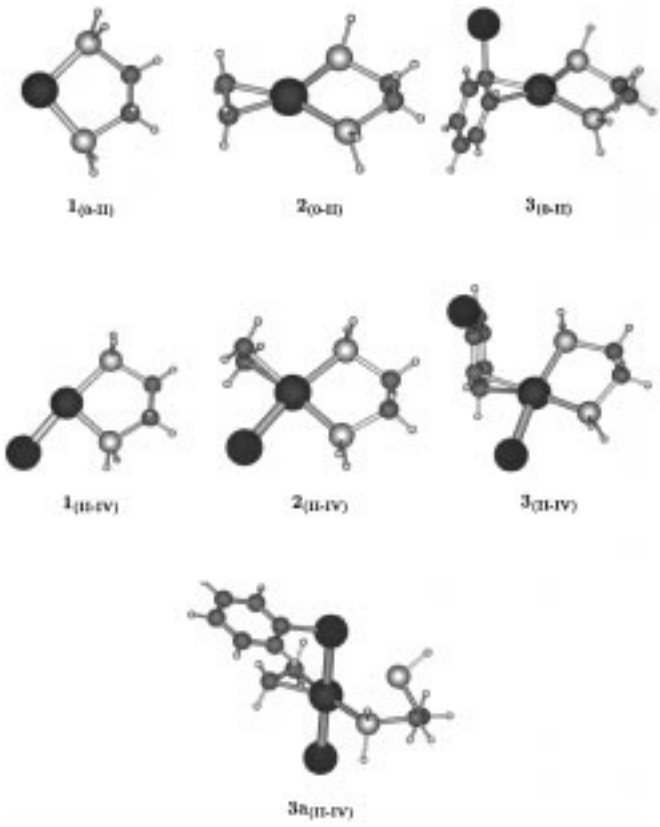

Figure 2. Complexes formed by $\mathbf{1}_{(0\text{-}II)}$ and $\mathbf{1}_{(II\text{-}IV)}$ with ethylene and/or phenyl iodide. These complexes are relevant as entry channels for the Heck reaction.

$\approx 70\ kJ\,mol^{-1}$, implying that reaction temperatures in the experiment have to be high enough to ensure reversibility of the ethylene coordination and the formation of $\mathbf{3}_{(0\text{-}II)}$, which is—according to our calculations—the entry channel for C–I oxidative addition. The importance of ligand dissociation for the kinetics of this reaction step has been demonstrated by experimental studies by Amatore and Jutand on the oxidative addition of Ph–I to palladium(0) complexes with various ligands.[36, 37]

For the Pd^{II}/Pd^{IV} pathway the 14-electron complex $\mathbf{1}_{(II\text{-}IV)}$ is assumed to be the active catalyst. This tricoordinate species can be described as a fragment of a square-planar complex (which is a stable ligand field for a d^8 transition metal atom) with a vacant coordination site *cis* to the iodo ligand: P-Pd-I angles of 88.3° and 175.5° are found. The I–Pd bond is directed only 0.9° out of the P-Pd-P plane. Complex $\mathbf{1}_{(II\text{-}IV)}$ also has the ability to coordinate ethylene (to form $\mathbf{2}_{(II\text{-}IV)}$) or to form complexes with phenyl iodide ($\mathbf{3}_{(II\text{-}IV)}$). These two complexes have stabilisation energies comparable to the corresponding palladium(0) species (See Tables 1 and 2).

Oxidative addition of Ph-I: In the Pd^0/Pd^{II} system C–I bond cleavage starts with the formation of the η^2 complex $\mathbf{3}_{(0\text{-}II)}$ with the palladium atom coordinating to the C_{ipso}–C_{ortho} bond of the phenyl ring (see Figure 2). The Pd–C_{ipso} bond is calculated to be slightly shorter than the Pd–C_{ortho} bond (Pd–C_{ipso} = 2.184 and Pd–C_{ortho} = 2.295 Å), for electronic reasons (electron-withdrawing I atom on C_{ipso}). These bond lengths are comparable to those in the ethylene complex $\mathbf{2}_{(0\text{-}II)}$ (Pd–C_{Eth} = 2.193 Å).

Complex $\mathbf{3}_{(0\text{-}II)}$ is connected to the transition state $\mathbf{TS\text{-}3\text{-}4}_{(0\text{-}II)}$ on the energy hypersurface. Interestingly, this transition state is nonplanar (for a perspective view see Figure 3). The P-Pd-P and C-Pd-I planes are almost perpendicular (dihedral angle P-P-Pd-I = 116.7°). A discussion of this unexpected structure has been given by Sakaki et al.[38] for the oxidative addition of C–C and Si–C bonds to a Pt^0 complex. According to these authors, the nonplanarity of the transition state structure can only be attributed to steric factors. In contrast to experimental studies on the oxidative addition of aryl chlorides,[39] a population analysis (utilizing the NPA-partitioning scheme[40, 41] at the B3LYP/lanl2dz level) reveals no pronounced charge separation in this transition state. For $\mathbf{TS\text{-}3\text{-}4}_{(0\text{-}II)}$ a group charge of −0.3 was found for the phenyl ring; this value is very similar to the values found for $\mathbf{4}_{(0\text{-}II)}$ (−0.3) and phenyl iodide (−0.2). Thus, the reaction of phenyl iodide has more the character of a concerted bond cleavage rather than a nucleophilic aromatic substitution.

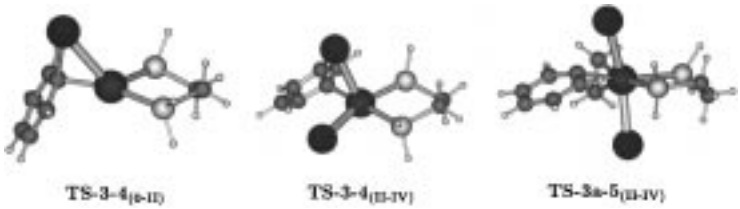

Figure 3. Perspective view of the transition states for the oxidative addition of phenyl iodide to Pd^0 or Pd^{II} complexes.

Our calculated barrier height implies that this oxidative addition is a rapid reaction step. (In this discussion all energies are calculated at the B3LYP/B_{large}//B3LYP/lanl2dz level unless noted otherwise.) The transition state $\mathbf{TS\text{-}3\text{-}4}_{(0\text{-}II)}$ is only 15.7 kJ mol^{-1} higher in energy than the corresponding η^2 complex of phenyl iodide $\mathbf{3}_{(0\text{-}II)}$ and, therefore, actually below the reactants in energy. Thus, for the Pd^0/Pd^{II} mechanism oxidative addition can be ruled out as the rate-determining step of the catalytic cycle. Instead, inhibition of the active catalyst due to alkene coordination may have an important impact on the reaction rate, because the high stability of $\mathbf{2}_{(0\text{-}II)}$ results in a low concentration of free $\mathbf{1}_{(0\text{-}II)}$ in the pre-equilibrium $\mathbf{1}_{(0\text{-}II)}$ + ethylene $\rightleftharpoons \mathbf{2}_{(0\text{-}II)}$.

As a product of the exothermic ($\Delta E = -141.8$ kJ mol^{-1}) and, therefore, presumably irreversible oxidative addition reaction, a square-planar palladium(II) complex $\mathbf{4}_{(0\text{-}II)}$ is formed. Due to the strong *trans* influence of the phenyl ligand, the Pd–P bond *trans* to the Pd–C bond becomes longer in comparison with $\mathbf{1}_{(0\text{-}II)}$ (Pd–P 2.515 Å), while the length of the other Pd–P bond is almost unchanged (Pd–P 2.411 Å). Our calculated Pd–C_{Ph} bond length of 2.035 Å corresponds to a palladium–carbon single bond. (For the carbene system a value of 2.06 Å has been reported.[35])

Table 1. Relative energies [in kJ mol^{-1}] for the Pd^0/Pd^{II} mechanism.

Structure	ΔE[a]	ΔE[b]	ΔE[c]	ΔE[d]	ΔG(298 K)[a]	ΔH(298 K)[a]
$\mathbf{1}_{(0\text{-}II)}$ + PhI + C_2H_4	0.0	0.0	0.0	0.0	0.0	0.0
$\mathbf{2}_{(0\text{-}II)}$ + PhI	−106.8	−97.0	−104.1	−115.2	−57.0	−101.7
$\mathbf{3}_{(0\text{-}II)}$ + C_2H_4	−46.3	−30.7	−31.5	−50.6	−1.4	−43.4
$\mathbf{TS\text{-}3\text{-}4}_{(0\text{-}II)}$ + C_2H_4	−36.5	−17.7	−15.8	−34.2	8.4	−35.8
$\mathbf{4}_{(0\text{-}II)}$ + C_2H_4	−154.7	−126.3	−141.8	−142.1	−105.1	−147.6
The following energies are relative to $\mathbf{5}_{(0\text{-}II)}$.						
$\mathbf{5}_{(0\text{-}II)}$	0.0	0.0	0.0	0.0	0.0	0.0
$\mathbf{TS\text{-}5\text{-}6}_{(0\text{-}II)}$	27.8	34.0	37.9	29.2	33.1	24.6
$\mathbf{6}_{(0\text{-}II)}$	−78.7	−76.9	−62.0	−90.4	−65.4	−74.5
$\mathbf{TS\text{-}6\text{-}7}_{(0\text{-}II)}$	−36.2	−38.4	−21.0	−42.2	−30.2	−37.6
$\mathbf{7}_{(0\text{-}II)}$	−51.7	−57.4	−47.6	−63.8	−46.1	−52.8
$\mathbf{TS\text{-}7\text{-}8}_{(0\text{-}II)}$	−30.7	−40.7	−32.3	−43.9	−32.2	−40.6
$\mathbf{8}_{(0\text{-}II)}$	−43.4	−50.1	−41.2	−45.8	−44.2	−47.9
$\mathbf{9}_{(0\text{-}II)}$ + styrene	94.6	79.3	88.6	96.9	40.6	83.5

[a] B3LYP/lanl2dz. [b] B3LYP/lanl2dz + p//B3LYP/lanl2dz. [c] B3LYP/B_{large}//B3LYP/lanl2dz. [d] mPW1PW91/lanl2dz + p//B3LYP/lanl2dz.

Table 2. Relative energies [in kJ mol^{-1}] for the Pd^{II}/Pd^{IV} mechanism. As origin of the energy scale we chose $\mathbf{1}_{(II\text{-}IV)}$ + PhI + ethylene.

Structure	ΔE[a]	ΔE[b]	ΔE[c]	ΔE[d]	ΔG(298 K)[a]	ΔH(298 K)[a]
$\mathbf{1}_{(II\text{-}IV)}$ + C_2H_4 + PhI	0.0	0.0	0.0	0.0	0.0	0.0
$\mathbf{3}_{(II\text{-}IV)}$ + C_2H_4	−81.7	−76.0	−69.5	−93.0	−2.4	−51.9
$\mathbf{TS\text{-}3\text{-}4}_{(II\text{-}IV)}$ + C_2H_4	38.9	67.5	70.8	56.9	92.3	39.1
$\mathbf{4a}_{(II\text{-}IV)}$ + C_2H_4	19.4	49.1	47.0	37.6	70.3	22.1
$\mathbf{4c}_{(II\text{-}IV)}$ + C_2H_4	34.9	67.6	71.1	58.7	79.2	36.8
$\mathbf{4d}_{(II\text{-}IV)}$ + C_2H_4	41.6	59.9	57.3	44.2	95.2	45.4
$\mathbf{2}_{(II\text{-}IV)}$ + PhI	−109.7	−99.6	−88.0	−116.0	−58.3	−103.3
$\mathbf{3a}_{(II\text{-}IV)}$	−80.8	−64.4	−47.8	−85.4	8.3	−70.5
$\mathbf{TS\text{-}3a\text{-}5}_{(II\text{-}IV)}$	44.0	66.4	84.0	39.8	146.0	50.9
$\mathbf{5a}_{(II\text{-}IV)}$	0.3	28.8	35.8	3.6	102.9	10.3
$\mathbf{5b}_{(II\text{-}IV)}$	2.9	22.9	24.8	−16.0	116.3	15.7
$\mathbf{5c}_{(II\text{-}IV)}$	6.5	37.8	48.3	7.4	114.0	17.0
$\mathbf{5d}_{(II\text{-}IV)}$	−32.3	−6.3	0.9	−43.8	79.8	−19.7
$\mathbf{TS\text{-}5\text{-}6}_{(II\text{-}IV)}$	−9.5	25.3	35.8	−15.8	105.5	0.4
$\mathbf{6}_{(II\text{-}IV)}$	−130.1	−102.0	−81.2	−150.5	−7.9	−114.0
$\mathbf{TS\text{-}6\text{-}7}_{(II\text{-}IV)}$	−86.3	−65.8	−50.3	−103.8	29.9	−75.2
$\mathbf{7}_{(II\text{-}IV)}$	−105.0	−82.4	−70.3	−122.9	5.2	−93.5
$\mathbf{TS\text{-}7\text{-}8}_{(II\text{-}IV)}$	−90.5	−69.5	−56.8	−109.4	15.0	−88.7
$\mathbf{8}_{(II\text{-}IV)}$	−113.8	−90.3	−76.4	−119.7	−8.8	−106.3
$\mathbf{9}_{(II\text{-}IV)}$ + styrene	28.5	33.6	31.6	22.3	70.6	28.4

[a] B3LYP/lanl2dz. [b] B3LYP/lanl2dz + p//B3LYP/lanl2dz. [c] B3LYP/B_{large}//B3LYP/lanl2dz. [d] mPW1PW91/lanl2dz + p//B3LYP/lanl2dz.

0947-6539/01/0708-1706 $ 17.50+.50/0 *Chem. Eur. J.* **2001**, *7*, No. 8

In order to initiate the C–C coupling reaction, an alkene has to coordinate in a position *cis* to the phenyl ligand. Because the palladium(II) complex is coordinatively saturated, an axial coordination is impossible. Therefore, previous ligand dissociation is necessary to provide a vacant coordination site. We verified this by performing optimisations on several pentacoordinated species (with ethylene as the fifth ligand). None of our attempts led to a minimum with a pentacoordinated palladium centre; the energy surface was rather found to be dissociative with respect to the loss of one ligand.

For our model calculations we chose to replace the iodo ligand by the alkene—forming a cationic complex—to allow a comparison with the reaction steps in the Pd^{II}/Pd^{IV} system, which also bears a positive charge. In principle, phosphine detachment could also be considered, but since the dissociation into ions is strongly solvent dependent, a decision on whether Pd–I or Pd–P cleavage is more facile lies beyond the scope of this computational study. However, we note that reference [35] favours I^- cleavage over Pd–P cleavage; this buttresses our decision to consider exclusively the path following I^- release. This reaction path should likewise be favoured by a polar solvent. The replacement of I^- with ethylene has only minor influence on the other bond lengths (Pd–P 2.535 and 2.389 Å respectively), an indication that I^- and C_2H_4 have a comparable *trans* influence.

For the Pd^{II}/Pd^{IV} pathway the mechanism of the oxidative addition step is much less straightforward to derive. There are two possibilities: a) complex $\mathbf{1}_{(II–IV)}$ reacts analogously to $\mathbf{1}_{(0–II)}$ but involves the formation of a pentacoordinate intermediate or b) the alkene coordinates in the first step and oxidative addition occurs afterwards. Both pathways lead to a octahedral Pd^{IV} complex as depicted in Scheme 4.

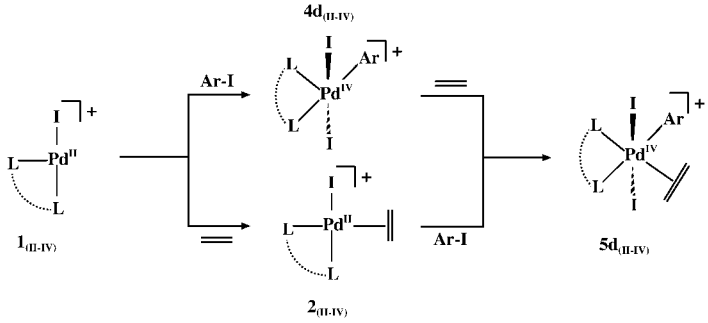

Scheme 4. Alternate pathways for the oxidative addition step.

For this study we took both pathways into account and calculated the relevant stationary points for both reactions. If the oxidative addition is assumed to be the first step of the formation of the octahedral complex, $\mathbf{3}_{(II-IV)}$ is determined as a probable entry complex (for a perspective view of the molecular structure see Figure 2). This structure can be understood as a distorted η^2 complex of the Pd centre with the C_2–C_3 bond of the phenyl ring (Pd–C_2 = 2.432 Å, Pd–C_3 = 2.639 Å).

Upon C–I bond cleavage four isomers are possible (permutations of the phenyl ligand and the vacant coordination site). Three of them are depicted in Figure 4 (top row).

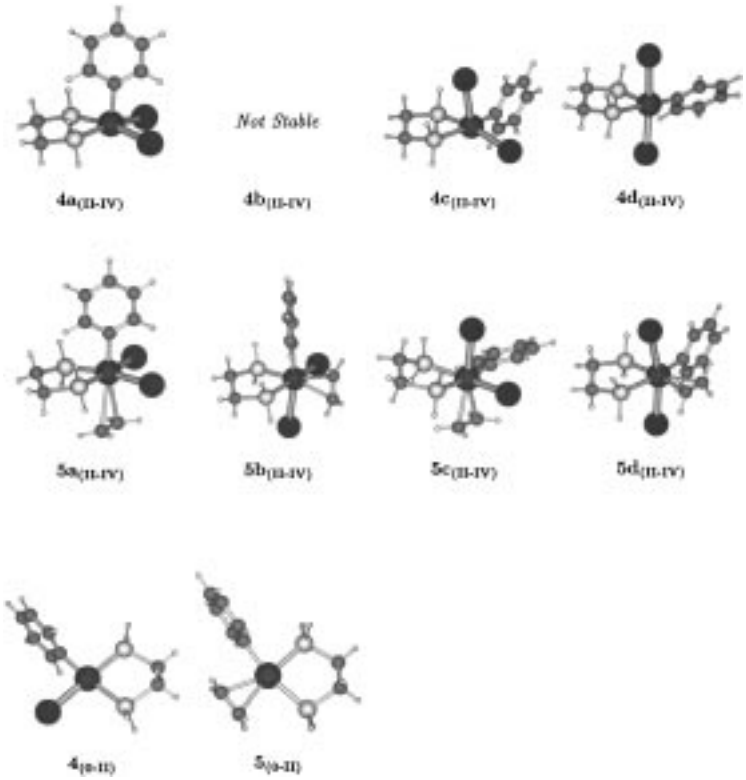

Figure 4. Perspective view of the three stable isomers of $[Pd(dpe)I_2Ph]^+$ (top) and the four isomers of $[Pd(dpe)(C_2H_4)I_2Ph]^+$ (middle) in comparison with the oxidative addition product of the Pd^0 complex (bottom). For the relative stabilities of these structures see Table 2.

The fourth one with the phenyl ligand in the axial position and the vacant coordination site in an equatorial position is not a minimum. Instead, a barrierless rearrangement to $\mathbf{4a}_{(II-IV)}$, the most stable isomer, occurs. The stability ordering of the structures (i.e., $\mathbf{4a}_{(II-IV)} > \mathbf{4c}_{(II-IV)} > \mathbf{4d}_{(II-IV)}$) can be rationalised in terms of the *trans* influence of the ligand in *trans* position of the vacant site in each case; this is expected to be largest for phenyl and smallest for the phosphine ligand. All of the intermediates are unstable toward dissociation into the reactants ($\mathbf{1}_{(II-IV)}$ + I–Ph). The corresponding transition states are found very late on the reaction coordinate of the oxidative addition reaction. Apart from energetic considerations, this can also be verified by comparison of the structural parameters of **TS-3-4**$_{(II-IV)}$ and $\mathbf{4c}_{(II-IV)}$ (see Table 3), which are very similar. Reductive elimination of I–Ph from $\mathbf{4d}_{(II-IV)}$ $\mathbf{4c}_{(II-IV)}$ is a fast process, making the existence of this intermediate questionable.

Table 3. Optimised structural data [in Å] for the stationary points of the oxidative addition of Ph–I (at the B3LYP/lanl2dz level).

Structure	Pd–P	Pd–I	Pd–C	C–I
TS-3-4$_{(0-II)}$	2.467, 2.602	2.949	2.128	2.330
$\mathbf{3}_{(0-II)}$	2.411, 2.515	2.685	2.035	3.378
TS-3-4$_{(II-IV)}$	2.463, 2.531	2.702	2.094	3.113
$\mathbf{4c}_{(II-IV)}$	2.454, 2.599	2.646	2.068	3.472
TS-3a-5$_{(II-IV)}$	2.408, 2.913	2.755	2.316	2.622
$\mathbf{5d}_{(II-IV)}$	2.382, 2.587	2.780	2.171	3.720

According to our calculations, the mechanism that involves $\mathbf{2}_{(II\text{-}IV)}$ seems to be a more realistic alternative. Complex $\mathbf{2}_{(II\text{-}IV)}$ is able to form complex $\mathbf{3a}_{(II\text{-}IV)}$ (see Figure 2), in which I–Ph is coordinated through a Pd–I interaction (Pd–I = 2.846 Å). Due to phosphine detachment (Pd–P = 2.433 Å and 3.140 Å, respectively) the palladium coordination remains square planar (as one would expect for a d^8 complex). Because the Pd–P bond is stronger than the Pd–I bond to the phenyl bound iodine, this coordination reaction is endoenergetic by 40.2 kJ mol^{-1}.

The entry complex $\mathbf{3a}_{(II\text{-}IV)}$ is connected to a transition state for C–I bond cleavage **TS-3a-5**$_{(II\text{-}IV)}$ (see Figure 3); this leads to an hexacoordinate intermediate with the two iodo ligands in the axial positions. In the course of the oxidative addition via a three-centred (Pd-I-C) transition state, the phosphine attaches simultaneously to the palladium centre. For the transition state a P–Pd bond length of 2.913 Å is found for this phosphine group; for the other one the bond length is much shorter (2.408 Å). The intermediate structure $\mathbf{5a}_{(II\text{-}IV)}$ has more symmetrical Pd–P bond lengths of 2.587 Å and 2.382 Å, respectively. This difference is comparable to $\mathbf{5}_{(0\text{-}II)}$ and can be explained by the *trans* influence of the ethylene and the phenyl ligand. Interestingly, the Pd–I bond length does not change greatly in the course of the oxidative addition. Instead, the Pd–C bond length decreases significantly on going from **TS-3a-5**$_{(II\text{-}IV)}$ to $\mathbf{5d}_{(II\text{-}IV)}$, which is in contrast to the Pd^0/Pd^{II} mechanism in which both the Pd–I and the Pd–C bond lengths become significantly smaller upon the C–I bond cleavage. This finding can be attributed to the more polar character of the transition state in the Pd^{II}/Pd^{IV} reaction.

Our calculations give evidence that the oxidative addition step in the Pd^{II}/Pd^{IV} catalytic cycle is preceded by an additional, simultaneous change in the coordination number of the palladium centre. This finding is supported by experimental and theoretical results for the reductive elimination reaction (the "reverse counterpart" of the oxidative addition) from Pt^{IV} complexes[42, 43] or Rh^{III} complexes.[44, 45] For this reaction, ligand dissociation (reducing the coordination number to five) was found to be favoured prior to the reductive elimination. Because of the importance of intermediate ligand detachment, we expect that this reaction step is promoted by a bidentate ligand with one weakly coordinating group, which allows facile change of the coordination number. In contrast, the oxidative addition is the rate-determining step for the Pd^{II}/Pd^{IV} mechanism (possibly in competition with the final dissociation step, depending on the solvent), while it is fast in the case of the Pd^0/Pd^{II} pathway.

Once a hexacoordinate Pd^{IV} species is formed, the Heck reaction can proceed. For the sake of completeness, we optimised the structures of all four possible isomers. The relative stability of the complexes decreases in the order $\mathbf{5d}_{(II\text{-}IV)} > \mathbf{5a}_{(II\text{-}IV)} > \mathbf{5b}_{(II\text{-}IV)} > \mathbf{5c}_{(II\text{-}IV)}$. Thus, the most stable isomer ($\mathbf{5d}_{(II\text{-}IV)}$) with the phenyl ligand and the alkene occupying equatorial positions is the one resulting from our proposed oxidative addition pathway. With the intermediates $\mathbf{5d}_{(II\text{-}IV)}$ and $\mathbf{5}_{(0\text{-}II)}$ being qualitatively very similar for all further steps of the catalytic cycle, equivalent stationary points have to be expected.

The alkene insertion step: In order to be able to compare the two reaction pathways, we chose the qualitatively equivalent intermediates $\mathbf{5}_{(0\text{-}II)}$ and $\mathbf{5d}_{(II\text{-}IV)}$ as the origin of our energy scale for the discussion of all subsequent reaction steps. An energy profile of these reaction steps is depicted in Figure 5.

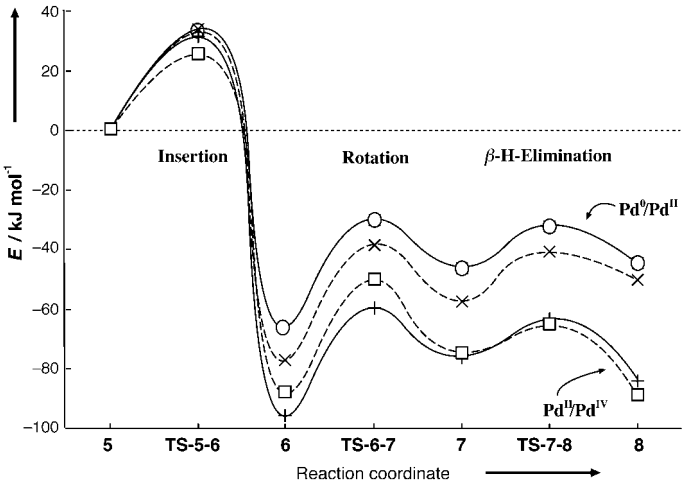

Figure 5. The calculated relative energies reveal that the energy hypersurfaces for the two alternative reaction mechanisms are essentially parallel (Energies are given relative to $\mathbf{5}_{(0\text{-}II)}$ and $\mathbf{5d}_{(II\text{-}IV)}$, respectively). ○: $\Delta E(Pd^0/Pd^{II})$; ×: $\Delta G_{298\,K}(Pd^0/Pd^{II})$; +: $\Delta E(Pd^{II}/Pd^{IV})$; □: $\Delta G_{298\,K}(Pd^{II}/Pd^{IV})$. For the exact energetic data see Tables 1 and 2. A perspective view of the corresponding molecular structures is given in Figure 6.

Starting from $\mathbf{5}_{(0\text{-}II)}$ the ethylene can insert into the Pd–C_{ar} bond. This reaction proceeds via a four-centred transition state **TS-5-6**$_{(0\text{-}II)}$, which involves the breaking of the Pd–C_β and Pd–C_{ar} bonds and the concerted C_β–C_{ar} bond formation (see Figure 6). The most pronounced structural changes in comparison with $\mathbf{5}_{(0\text{-}II)}$ are the shortening of the Pd–C_α bond by 0.232 Å (an indication of the formation of a Pd–C σ bond) and the reduced C_β–C_{ar} distance accompanied by a bending of the phenyl ring by approximately 30° (due to the C–C bond formation). Our calculated barrier height of 37.9 kJ mol^{-1} is very similar to the value found for the system with carbene ligands (34.3 kJ mol^{-1}),[35] indicating that the choice of the ligand system has only a minor effect on this reaction step. Activation energies of comparable magnitude have been calculated for ethylene insertions into transition-metal–methyl bonds (for a collection of computed data on this topic the reader is referred to a recent review by Niu and Hall[46]).

Through the ethylene insertion, the alkyl complex $\mathbf{6}_{(0\text{-}II)}$ is formed as an intermediate. This structure is stabilised owing to an intramolecular interaction of the vacant coordination site of the Pd^{II} centre and the π system of the phenyl ring. The palladium carbon bond lengths Pd–C_{ipso} = 2.374, Pd–C_{ortho} = 2.667, and Pd–C'_{ortho} = 3.052 Å may be interpreted as a distorted η^2 interaction. Albert et al. found a similar arrangement, although in their system the η^2 interaction is more symmetric (Pd–C_{ipso} = 2.48 and Pd–C_{ortho} = 2.55 Å).[35] Complex $\mathbf{6}_{(0\text{-}II)}$ was calculated to be 62.0 kJ mol^{-1} more stable than the ethylene complex $\mathbf{5}_{(0\text{-}II)}$; this is comparable to an exothermicity of 64.4 kJ mol^{-1} found in the case of the carbene stabilised system.[35]

0947-6539/01/0708-1708 $ 17.50+.50/0 *Chem. Eur. J.* **2001**, *7*, No. 8

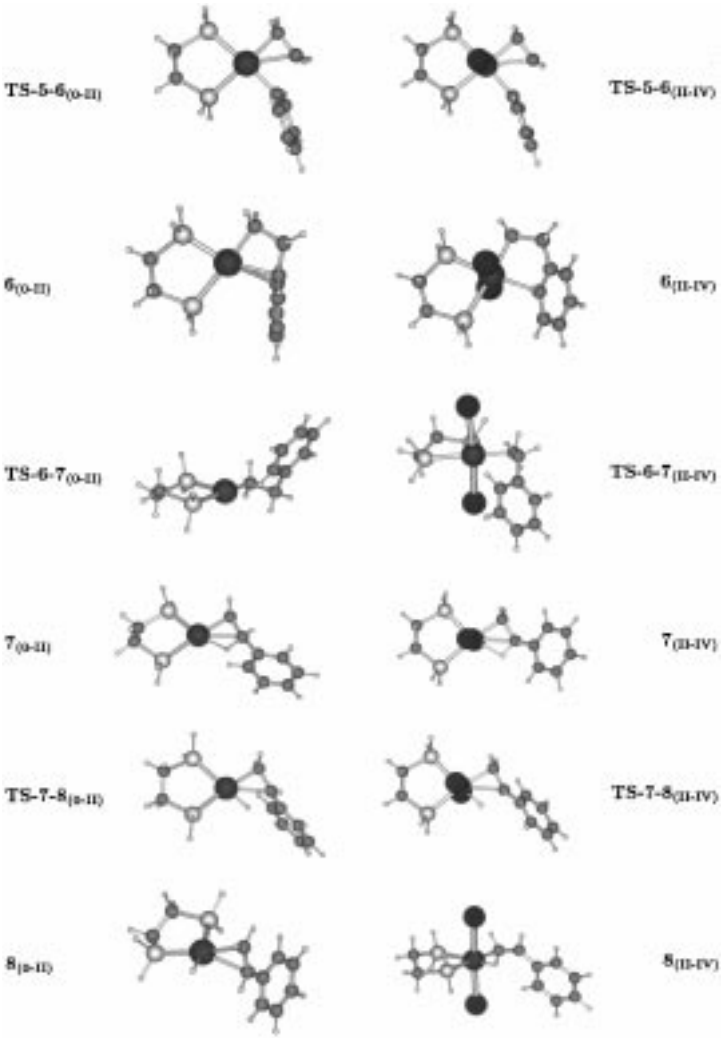

Figure 6. Perspective view of all stationary points involved in the conversion of $\mathbf{5}_{(0\text{-II})}$ and $\mathbf{5}_{(\text{II-IV})}$ into the product complexes $\mathbf{8}_{(0\text{-II})}$ and $\mathbf{8}_{(\text{II-IV})}$. For selected structural parameters see Table 4 or in the text. The complete set of Cartesian coordinates for all stationary points is available as supplementary material.

Table 4. Selected structural data [in Å] for some stationary points of the insertion/elimination pathway (optimised at the B3LYP/lanl2dz level).

Structure	Pd–P	Pd–C_{Ph}	Pd–C_α	Pd–C_β
$\mathbf{5}_{(0\text{-II})}$	2.389, 2.535	2.074	2.389	2.406
$\mathbf{5a}_{(\text{II-IV})}$	2.460, 2.461	2.114	2.974	3.034
$\mathbf{5b}_{(\text{II-IV})}$	2.388, 2.478	2.175	2.484	2.442
$\mathbf{5c}_{(\text{II-IV})}$	2.483, 2.597	2.136	2.570	2.568
$\mathbf{5d}_{(\text{II-IV})}$	2.382, 2.587	2.171	2.455	2.444
$\mathbf{TS\text{-}5\text{-}6}_{(0\text{-II})}$	2.456, 2.483	2.143	2.157	2.468
$\mathbf{TS\text{-}5\text{-}6}_{(\text{II-IV})}$	2.476, 2.496	2.237	2.212	2.535
	Pd–P	Pd–H	Pd–C_α	Pd–C_β
$\mathbf{7}_{(0\text{-II})}$	2.385, 2.499	1.909	2.078	2.435
$\mathbf{7}_{(\text{II-IV})}$	2.381, 2.542	2.056	2.135	2.549
$\mathbf{TS\text{-}7\text{-}8}_{(0\text{-II})}$	2.430, 2.467	1.614	2.167	2.455
$\mathbf{TS\text{-}7\text{-}8}_{(\text{II-IV})}$	2.473, 2.481	1.644	2.198	2.548
$\mathbf{8}_{(0\text{-II})}$	2.396, 2.549	1.556	2.281	2.447
$\mathbf{8}_{(\text{II-IV})}$	2.425, 2.566	1.552	2.266	2.839

For the Pd^{II}/Pd^{IV} mechanism, ethylene insertion also proceeds via a four-centred transition state. According to our calculations this reaction requires an activation energy of 34.9 kJ mol^{-1}, which is similar to the value found for the Pd^0/Pd^{II} system. An inspection of the graphical representation given in Figure 6 reveals the qualitative equivalence of $\mathbf{TS\text{-}5\text{-}6}_{(0\text{-II})}$ and $\mathbf{TS\text{-}5\text{-}6}_{(\text{II-IV})}$. This equivalence is also found in the calculated structural parameters (see Table 4).

In principle, the insertion could occur from all three isomers with the phenyl and the alkene ligand in *cis* position. According to our calculations, the corresponding activation barriers for the alkene insertion starting from $\mathbf{5b}_{(\text{II-IV})}$, $\mathbf{5c}_{(\text{II-IV})}$ and $\mathbf{5d}_{(\text{II-IV})}$ are all very similar (See Table 2). Because $\mathbf{5d}_{(\text{II-IV})}$ was found to be the most stable isomer and connected to a possible entry channel, we concentrated on the catalytic cycle involving this isomer.

The corresponding product of the alkene insertion reaction $\mathbf{6}_{(\text{II-IV})}$ is again stabilised by an interaction between the palladium centre and the phenyl ring. (At first sight, $\mathbf{6}_{(\text{II-IV})}$ would appear to be an η^2 complex, but the computed Wiberg bond indices[47] show no sign of appreciable bonding to the second ring carbon.) In contrast to $\mathbf{6}_{(0\text{-II})}$, the η^2 interaction is much more asymmetric, favouring a short Pd–C_{ortho} bond (Pd–C_{ipso} = 2.855, Pd–C_{ortho} = 2.441 Å). This can be rationalised by the repulsive interaction between the aryl hydrogen atoms and the iodo ligands, which is minimised due to the distortion. Because this repulsion is operative in $\mathbf{5d}_{(\text{II-IV})}$ and $\mathbf{TS\text{-}5\text{-}6}_{(\text{II-IV})}$, the relative stabilisation of $\mathbf{6}_{(\text{II-IV})}$ is larger than for $\mathbf{6}_{(0\text{-II})}$ ($\Delta E = -82.1$ kJ mol^{-1}). This is also witnessed by the increase of the I-Pd-I angle from 165.6° in $\mathbf{5d}_{(\text{II-IV})}$ to 172.3° in $\mathbf{6}_{(0\text{-II})}$.

The β-hydride elimination: In order to release the desired product of the Heck reaction (i.e., styrene in the case of our model) a β-hydride elimination is necessary (see Scheme 2). For the reaction the Pd–C_α and the corresponding C_β–H bond have to be in *cis* position. This can be achieved by a rotation of the coordinated alkane around the C_α–C_β bond involving the transition state $\mathbf{TS\text{-}6\text{-}7}_{(0\text{-II})}$. Because in $\mathbf{TS\text{-}6\text{-}7}_{(0\text{-II})}$ the interaction of the palladium atom with the phenyl ring is no longer stabilising the system, this rotation requires an activation energy of 41.0 kJ mol^{-1}. More than half of it (26.6 kJ mol^{-1}) is released upon the formation of a β-agostic complex $\mathbf{7}_{(0\text{-II})}$ (which is therefore 14.4 kJ mol^{-1} less stable than $\mathbf{6}_{(0\text{-II})}$). Due to the agostic interaction, the C_β–H bond becomes weaker (e.g., the C–H bond length for the interacting bond is found 0.1 Å larger than for the noninteracting one). Thus, facile cleavage of the C–H bond is possible. The calculated activation barrier for the β-hydride elimination is only 15.3 kJ mol^{-1} (relative to $\mathbf{7}_{(0\text{-II})}$): the transition state $\mathbf{TS\text{-}7\text{-}8}_{(0\text{-II})}$ is even slightly lower in energy than $\mathbf{TS\text{-}6\text{-}7}_{(0\text{-II})}$. This finding reveals that the major part of the barrier for the β-hydride elimination step results from breaking the Pd–C_{Ph} bond. Due to this intramolecular stabilisation of $\mathbf{6}_{(0\text{-II})}$ the elimination step leading to the product complex $\mathbf{8}_{(0\text{-II})}$ is endoenergetic by 20.8 kJ mol^{-1}. The overall insertion/elimination reaction is exoenergetic by 41.2 kJ mol^{-1}; for the carbene stabilised system 37.2 kJ mol^{-1} have been reported. A comparison with

the results obtained by Albert et al.[35] reveals that the barriers involved in the insertion and the subsequent β-hydride elimination differ only slightly between a carbene- and a phosphine-stabilised palladium centre.

Compounds $\mathbf{8}_{(0\text{-}II)}$ and $\mathbf{7}_{(0\text{-}II)}$ are found to have almost the same energy, that is, the barrier between the isomers is small, and the following step has a high barrier. Therefore one can expect a considerable lifetime of the system in conformation **7**. Hence our results support a mechanism proposed by Deeth et al.,[48] who considered a direct abstraction of the agostic proton (in $\mathbf{7}_{(0\text{-}II)}$) by the auxiliary base present in the reaction mixture without formation of the palladium hydride species $\mathbf{8}_{(0\text{-}II)}$. According to our calculations, the β-hydride elimination is reversible and an intermolecular reaction of $\mathbf{7}_{(0\text{-}II)}$ cannot be ruled out.

Also in the course of the Pd^{II}/Pd^{IV} reaction the bond between the palladium atom and the phenyl ring has to be broken to bring the β-hydrogen atom into an appropriate position for the elimination step. Again, the transition state for this rotation $\mathbf{TS\text{-}6\text{-}7}_{(II\text{-}IV)}$ is higher than the transition state for the β-hydride elimination $\mathbf{TS\text{-}7\text{-}8}_{(II\text{-}IV)}$ itself (the rotation requires 30.9 kJ mol^{-1}, the elimination 13.5 kJ mol^{-1} relative to the corresponding intermediates). Because the rotation involves a large amplitude motion of the alkyl ligand (first the Pd–C–C angle has to become larger, then the 120° rotation around the C–C bond occurs and finally the Pd-C-C angle becomes smaller again) the potential energy hypersurface in this region is very flat, which makes the calculation of an intrinsic reaction coordinate difficult (i.e., a small step size is required). Nevertheless, we could verify that $\mathbf{TS\text{-}6\text{-}7}_{(II\text{-}IV)}$ connects $\mathbf{6}_{(II\text{-}IV)}$ with a β-H-agostic intermediate $\mathbf{7}_{(II\text{-}IV)}$ on the energy hypersurface. As in the Pd^0/Pd^{II} mechanism $\mathbf{7}_{(II\text{-}IV)}$ precedes the β-hydride elimination step. Because of the higher electrophilicity of the Pd^{IV} centre, the elimination step is even more facile than for the Pd^0/Pd^{II} pathway. Overall, the insertion/elimination step starting from $\mathbf{5d}_{(II\text{-}IV)}$ is exothermic by 75.5 kJ mol^{-1}.

In the product complex $\mathbf{8}_{(II\text{-}IV)}$ the styrene is bound very asymmetrically. The palladium atom interacts with one carbon atom of the styrene molecule only (Pd–C_α = 2.266, Pd–C_β = 2.839 Å). To elucidate the reason for this distortion, we performed additional calculations on a system in which the coordinating styrene is replaced by ethylene. Since this complex is found to be symmetric (Pd–C_α = 2.369, Pd–C_β = 2.420 Å), we assume that the distortion is caused by the repulsive interaction between the phenyl group and one of the axial iodo ligands. This interaction also results in systematically longer Pd–C_β bond lengths for the Pd^{II}/Pd^{IV} reaction relative to the Pd^0/Pd^{II} reaction, while the Pd–C_α bond lengths are almost equal (see Table 4).

In $\mathbf{8}_{(0\text{-}II)}$ as well as in $\mathbf{8}_{(II\text{-}IV)}$, the styrene molecule forms a stable complex with the palladium centre. The dissociation into free styrene and the corresponding complex fragments ($\mathbf{9}_{(0\text{-}II)}$ and $\mathbf{9}_{(II\text{-}IV)}$) is calculated to be strongly endothermic; according to the reaction $\mathbf{8}_{(0\text{-}II)} \rightarrow$ styrene + $\mathbf{9}_{(0\text{-}II)}$, the dissociation energy is 129.8 kJ mol^{-1} (108.0 kJ mol^{-1} for the Pd^{II}/Pd^{IV} pathway). Because the alkene dissociation is more facile from $\mathbf{2}_{(0\text{-}II)}$ and $\mathbf{2}_{(II\text{-}IV)}$ (104.1 and 88.0 kJ mol^{-1}, respectively) we assume that, at least in the gas phase, the reduction of the transition metal (probably by an intermolecular proton abstraction step involving the auxiliary base) is necessary prior to the styrene release. (This may not be the case in a polar solvent.)

Conclusion

A computational study on the Heck reaction by using density functional theory has been performed. Our results obtained at the B3LYP/B_{large}//B3LYP/lanl2dz level of theory can be summarised as follows:

1) The ethylene insertion and the β-H-elimination step require only small activation energies. Therefore, these steps have only minor importance for the overall reaction rate of the catalytic reaction. This holds true for the Pd^0/Pd^{II} as well as the Pd^{II}/Pd^{IV} pathway.
2) The hypothetical Pd^{II}/Pd^{IV} mechanism and the usual Pd^0/Pd^{II} mechanism for the Heck reaction involve qualitatively similar stationary points. In the Pd^{II}/Pd^{IV} case, the reaction takes place in the equatorial plane of an octahedral Pd^{IV} complex.
3) The Pd^{II}/Pd^{IV} mechanism has no intermediate dissociation step to provide a vacant coordination site for β-H-elimination.

According to our calculations, the dissociation steps necessary to provide vacant coordination sites (i.e., alkene dissociation from $\mathbf{2}_{(0\text{-}II)}$ and $\mathbf{8}_{(0\text{-}II)}$ and the iodide dissociation from $\mathbf{4}_{(0\text{-}II)}$) are likely to be rate-determining for the Pd^0/Pd^{II} mechanism. For the Pd^{II}/Pd^{IV} mechanism the oxidative addition of I–Ph is the step with the highest activation barrier. Because the oxidative addition occurs from a complex with a tetracoordinate palladium atom, a chelating ligand with one weak donor atom may reduce the activation barrier for this step. A study regarding this point is presently in progress in our laboratory.

Acknowledgement

J.M. is a Yigal Allon Fellow and the incumbent of the Helen and Milton A. Kimmelman Career Development Chair. A.S. gratefully acknowledges a postdoctoral fellowship of the MINERVA Foundation, Munich, Germany. O.U. is a doctoral fellow of the Feinberg Graduate School, Weizmann Institute of Science. This research was supported by the MINERVA foundation, Munich (Germany), and by the Tashtiyot program of the Ministry of Science (Israel). The Compaq ES40 server computer was jointly financed by the last two programs. The authors would like to thank Prof. David Milstein (Weizmann Institute) for helpful discussions and critical reading of the manuscript prior to submission, and Prof. Manfred Reetz (Max-Planck Institut für Kohlenforschung, Mülheim, Germany) for his encouragement.

[1] A. de Meijere, F. E. Meyer, *Angew. Chem.* **1994**, *106*, 2473–2505; *Angew. Chem. Int. Ed. Engl.* **1994**, *33*, 2379–2411.
[2] W. Cabri, I. Candiani, *Acc. Chem. Res.* **1995**, *28*, 2–7.
[3] I. P. Beletskaya, A. V. Cheprakov, *Chem. Rev.* **2000**, *100*, 3009–3066.
[4] W. A. Herrmann, C. Brossmer, K. Öfele, C.-P. Reisinger, T. Priermeier, M. Beller, H. Fischer, *Angew. Chem.* **1995**, *l07*, 1989–1992; *Angew. Chem. Int. Ed. Engl.* **1995**, *34*, 1844–1848.
[5] W. A. Herrmann, C. Brossmer, C.-P. Reisinger, T. H. Riermeier, K. Öffele, M. Beller, *Chem. Eur. J.* **1997**, *3*, 1357–1364.

0947-6539/01/0708-1710 $ 17.50+.50/0

[6] M. Ohff, A. Ohff, M. E. van der Boom, D. Milstein, *J. Am. Chem. Soc.* **1997**, *119*, 11 687 – 11 688.
[7] M. T. Reetz, G. Lohmer, R. Schwickardi, *Angew. Chem.* **1998**, *110*, 492 – 495; *Angew. Chem. Int. Ed.* **1998**, *37*, 481 – 483.
[8] B. L. Shaw, S. D. Perera, *Chem. Commun.* **1998**, 1863 – 1864.
[9] B. L. Shaw, S. D. Perera, E. A. Stanley, *Chem. Commun.* **1998**, 1361 – 1362.
[10] B. L. Shaw, *New J. Chem.* **1998**, 77 – 79.
[11] M. Ohff, A. Ohff, D. Milstein, *Chem. Commun.* **1999**, 357 – 358.
[12] W. A. Herrmann, V. P. W. Böhme, *J. Organomet. Chem.* **1999**, *572*, 141 – 145.
[13] K. Reddy, K. Surekha, G. H. Lee, S. M. Peng, S.-T. Liu, *Organometallics* **2000**, *19*, 2637 – 2639.
[14] J. M. Brunel, A. Heumann, G. Buono, *Angew. Chem.* **2000**, *112*, 2022 – 2025; *Angew. Chem. Int. Ed.* **2000**, *39*, 1946 – 1949.
[15] A. D. Becke, *J. Chem. Phys.* **1993**, *98*, 5648 – 5653.
[16] M. J. Frisch, G. W. Trucks, H. B. Schlegel, G. E. Scuseria, M. A. Robb, J. R. Cheeseman, V. G. Zakrzewski, J. A. Montgomery, Jr., R. E. Stratmann, J. C. Burant, S. Dapprich, J. M. Millam, A. D. Daniels, K. N. Kudin, M. C. Strain, O. Farkas, J. Tomasi, V. Barone, M. Cossi, R. Cammi, B. Mennucci, C. Pomelli, C. Adamo, S. Clifford, J. Ochterski, G. A. Petersson, P. Y. Ayala, Q. Cui, K. Morokuma, D. K. Malick, A. D. Rabuck, K. Raghavachari, J. B. Foresman, J. Cioslowski, J. V. Ortiz, B. B. Stefanov, G. Liu, A. Liashenko, P. Piskorz, I. Komaromi, R. Gomperts, R. L. Martin, D. J. Fox, T. Keith, M. A. Al-Laham, C. Y. Peng, A. Nanayakkara, C. Gonzalez, M. Challacombe, P. M. W. Gill, B. Johnson, W. Chen, M. W. Wong, J. L. Andrés, C. Gonzalez, M. Head-Gordon, E. S. Replogle, J. A. Pople, *Gaussian 98*, Revision A.7, Gaussian, Pittsburgh PA, **1998**.
[17] P. J. Hay, W. R. Wadt, *J. Chem. Phys.* **1985**, *82*, 270 – 283.
[18] W. R. Wadt, P. J. Hay, *J. Chem. Phys.* **1985**, *82*, 284 – 298.
[19] P. J. Hay, W. R. Wadt, *J. Chem. Phys.* **1985**, *82*, 299 – 310.
[20] T. H. Dunning, Jr., P. J. Hay in *Modern Theoretical Chemistry* (Ed.: H. F. Schaefer III), Plenum, New York, **1976**.
[21] C. Gonzalez, H. B. Schlegel, *J. Phys. Chem.* **1990**, *94*, 5523 – 5527.
[22] A. Höllwarth, M. Böhme, S. Dapprich, A. W. Ehlers, A. Gobbi, V. Jonas, K. F. Köhler, R. Stegmann, A. Veldkamp, G. Frenking, *Chem. Phys. Lett.* **1993**, *208*, 237 – 240.
[23] A. W. Ehlers, M. Böhme, S. Dapprich, A. Gobbi, A. Höllwarth, V. Jonas, K. F. Köhler, R. Stegmann, A. Veldkamp, G. Frenking, *Chem. Phys. Lett.* **1993**, *208*, 111 – 114.
[24] T. H. Dunning, Jr., *J. Chem. Phys.* **1989**, *90*, 1007 – 1023.
[25] D. E. Woon, T. H. Dunning, Jr., *J. Chem. Phys.* **1993**, *98*, 1358 – 1371.
[26] E. R. Davidson, *Chem. Phys. Lett.* **1996**, *260*, 3 – 4.
[27] D. Andrae, U. Haussermann, M. Dolg, H. Stoll, H. Preuss, *Theor. Chim. Acta* **1990**, *77*, 123 – 141.
[28] A. Bergner, M. Dolg, W. Küchle, H. Stoll, H. Preuss, *Mol. Phys.* **1993**, *80*, 1431 – 1441.
[29] H.-J. Werner, P. J. Knowles, J. Almlöf, R. D. Amos, A. Berning, D. L. Cooper, M. J. O. Deegan, A. J. Dobbyn, F. Eckert, S. T. Elbert, C. Hampel, R. Lindh, A. W. Lloyd, W. Meyer, A. Nicklass, K. Peterson, R. Pitzer, A. J. Stone, P. R. Taylor, M. E. Mura, P. Pulay, M. Schütz, H. Stoll, T. Thorsteinsson, *Molpro 98.1*, **1998**.
[30] M. N. Glukhovtsev, R. D. Bach, A. Pross, L. Radom, *Chem. Phys. Lett.* **1996**, *260*, 558 – 564.
[31] C. Adamo, V. Barone, *J. Chem. Phys.* **1998**, *108*, 664 – 675.
[32] J. M. L. Martin, C. W. Bauschlicher, A. Ricca, *Comput. Phys. Commun.* **2001**, *133*, 189 – 201.
[33] For more information about these grids see: Gaussian 98 Users Manual or its on-line version (URL: http://www.gaussian.com/techinfo.htm).
[34] G. Schaftenaar, "Molden 3.6", **1999**; URL: http://www.cmbi.kun.nl/~schaft/molden/molden.html.
[35] K. Albert, P. Gisdakis, N. Rösch, *Organometallics* **1998**, *17*, 1608 – 1616.
[36] C. Amatore, A. Jutand, *Coord. Chem. Rev.* **1998**, *178 – 180*, 511 – 528.
[37] C. Amatore, A. Fuxa, A. Jutand, *Chem. Eur. J.* **2000**, *6*, 1474 – 1482.
[38] S. Sakaki, N. Mizoe, Y. Musashi, B. Biswas, M. Sugimoto, *J. Phys. Chem. A* **1998**, *102*, 8027 – 8036.
[39] M. Portnoy, D. Milstein, *Organometallics* **1993**, *12*, 1665 – 1673.
[40] A. E. Reed, R. B. Weinstock, F. Weinhold, *J. Chem. Phys.* **1985**, *83*, 735 – 746.
[41] A. E. Reed, L. A. Curtiss, F. Weinhold, *Chem. Rev.* **1988**, *88*, 899 – 926.
[42] D. M. Crumpton, K. I. Goldberg, *J. Am. Chem. Soc.* **2000**, *122*, 962 – 963.
[43] K. L. Bartlett, K. I. Goldberg, W. T. Borden, *J. Am. Chem. Soc.* **2000**, *122*, 1456 – 1465.
[44] D. Milstein, *Acc. Chem. Res.* **1984**, *17*, 221 – 226.
[45] A. Sundermann, O. Uzan, D. Milstein, J. M. L. Martin, *J. Am. Chem. Soc.* **2000**, *122*, 7095 – 7104.
[46] S. Niu, M. B. Hall, *Chem. Rev.* **2000**, *100*, 353 – 405.
[47] K. B. Wiberg, *Tetrahedron* **1968**, *24*, 1083 – 1096.
[48] R. J. Deeth, A. Smith, K. K. M. Hii, J. M. Brown, *Tetrahedron Lett.* **1998**, *39*, 3229 – 3232.

Received: August 15, 2000 [F2675]